Instrument Science Report COS 2023-19(v1)

Focusing on New COS FUV Lifetime Positions: G130M/1222 and G160M at LP6

Fischer, T.C.[1], Fischer, W.J.[1], Frazer, E.[1], Indriolo, N.[1], James, B.[1], Johnson, C.I.[1], Plesha, R.[1], Rafelski, M.[1], Roman-Duval, J.[1], Rowlands, K.[1], Sahnow, D.[1]

[1] Space Telescope Science Institute, Baltimore, MD

7 August 2023

ABSTRACT

In the final two weeks of 2021, focus sweeps for the Lifetime Position 6 (LP6) were performed at a +6.5" sky offset with the G130M and G160M gratings through HST Program 16850. The focus sweeps were performed on the subdwarf B star Feige 48 at a range of focus settings. An auto-correlation technique was used to find the minimal line widths of absorption lines and therefore find the optimal focus for each setting. The final, absolute focus values for G130M/1222 and G160M/1600 are -881 steps and +108 steps, respectively.

Contents

1. Introduction

The location where spectra fall on the Cosmic Origins Spectrograph (COS) far-ultraviolet (FUV) detector is changed in the cross-dispersion direction (locations known as lifetime positions, LPs) to compensate for a reduction in modal gain with time. The optimal focus of the spectrograph, which minimizes the width of the astigmatic point spread function (PSF) along the dispersion direction, depends on lifetime position (LP), grating, and central wavelength (cenwave). We move Optics Select Mechanism 1 (OSM1) a number of focus steps to correct for this. By performing focus sweep programs, we can determine the best focus values at each LP, with the resultant focus values stored in an onboard flight software table. Zero-point focus values at LP6, estimated from foci across previous lifetime positions, were derived from results of the exploratory LP6 focus sweep (Fischer et al. 2022) at +7.0" in the cross-dispersion direction from LP1. This ISR presents the results of Program 16850, developed to obtain final focus values for all G160M cenwaves and G130M/1222 at +6.5", the final position for Lifetime Position 6 (LP6; James et al., 2023). As focus values at each lifetime position are grating- and cenwave-dependent, we perform a separate focus sweep for each grating for a single cenwave, as there are fixed, LP independent, focus offsets between cenwaves that are applied based on our analyses. Similar analyses of focus sweeps are described by Lennon et al. (2010) and Ghavamian et al. (2012) at LP1, Oliveira et al. (2013) at LP2, Fox et al. (2015) at LP3, Fox et al. (2017), Sonnentrucker et al. (2017), Sankrit et al. (2019), and James et al. (2019) at LP4, Fischer et al. (2021) at LP5, and Fischer et al. (2022) exploring LP6.

To perform a focus sweep, a star exhibiting multiple photospheric absorption lines is observed at numerous focus positions bracketing the estimated focus value. Then, a spectral line-width analysis is conducted to determine which position yields the sharpest absorption line features (i.e. which spectrum is best in focus). If the focus value that produces the sharpest absorption features is offset from the expected focus value, then a correction is applied to the expected value. The new, updated value is then included in the pcmech_OSMTbl table in the COS flight software. Ideally, these observations and analyses would be performed for each grating/cenwave combination for the G160M grating that will also be used at LP6. However, as described above, the focus offsets between cenwaves are constant. Therefore, we only measure the focus for the 1600 cenwave at the new lifetime position in this program and assume that the relative focus offset determined for this grating/cenwave combination is applicable to all cenwaves for the G160M grating, as successfully employed in previous sweep programs. Alternatively, for G130M/1222, it is the only G130M cenwave moved to

LP6, and therefore the only one requiring a focus sweep.

2. Observations

The sweeps performed in this program utilized COS/FUV observations with the G130M/1222 and G160M/1600 grating/cenwave setups for a total of 8 orbits across 2 visits. The target observed in this program is Feige 48, a subdwarf B star often chosen in previous sweep programs due to its low rotational velocity and plethora of narrow absorption lines (widths < 5 km s^{-1}) in the UV (Heber et al. 2000).

Observations were obtained in December of 2021 under Program ID 16850. Observations for both grating/cenwave set-ups employed a relative focus sweep from -1000 to +1000 steps across the estimated focus for each position in increments of 200 steps, with finer 100 step increments between -200 and +200 relative steps. Due to the brightness of Feige 48, the G130M sweeps were obtained separately for the FUVA and FUVB segments in order to avoid exceeding acceptable count rates. Tables 1 and 2 provide a list of the observations for each of the performed sweeps. The focus step columns in each table report, in order, 1) the relative focus sweep values at LP6, and 2) those same LP6 values corrected for telescope breathing, as discussed in Section 3.1.

3. Data Reduction

The data were reduced manually using the calibration pipeline `calcos` on the raw data files (`*rawtag*.fits`), as observations at LP6 were not supported by the automatic pipeline at the time the observations were taken. LP4 FLATFILE, SPOTTAB, and DISPTAB reference files were used for this manual reduction. The headers of the rawtag files were updated to change the FLATFILE keyword to `gw_imposter_flat.fits`, the grid-wire flat-field reference file. The manual reduction produced corrected events list files (`*corrtag*.fits`), which were corrected for thermal, geometric, and walk effects, and then converted into 2D images of counts read by the detector. From the 2D images, relevant rows were extracted with a boxcar weighting scheme and combined into 1D spectra. The extraction rows for each combination of grating, detector, and position offset are provided in Table 3. Wavelength arrays were created by manually applying a dispersion solution to the XFULL array, set to sufficiently approximate properly reduced data set wavelength ranges. Wavelength ranges for all observations follow COS instrument handbook specifications. FUVA and FUVB wavelength ranges for the G130M/1222 observations begin at 1220.0 and 1067.0 Å and proceed at 0.00996 Å per pixel and FUVA and FUVB wavelength ranges for the G160M/1600 observations begin at 1601.0 and 1409.0 Å and proceed in 0.01095 and 0.01088 Å increments, respectively.

Table 1. Log of exposures and focus offsets for G130M/1222 sweep across LP6.

Filename	Start Time (UT)	Relative Focus from LP6 (steps)	Breathing Corrected LP6 Focus (steps)
2021-12-21 – Estimated LP6 Absolute Focus : -951 steps			
FUVA			
lerl03h7q	05:54	-1000	-1033
lerl03h9q	05:59	-800	-846
lerl03heq	06:04	-600	-657
lerl03hgq	06:09	-400	-465
lerl03hiq	06:14	-200	-263
lerl03hkq	06:19	-100	-154
lerl03hmq	06:24	0	-55
lerl03hpq	06:29	+100	+53
lerl03hrq	06:34	+200	+160
lerl03htq	06:39	+400	+380
lerl03hvq	07:21	+600	+579
lerl03hxq	07:26	+800	+768
lerl03hzq	07:31	+1000	+956
FUVB			
lerl03i1q	07:45	+1000	+936
lerl03i3q	07:49	+800	+732
lerl03i5q	07:53	+600	+537
lerl03i7q	07:57	+400	+340
lerl03i9q	08:02	+200	+144
lerl03ibq	08:06	+100	+52
lerl03idq	08:10	0	-37
lerl03ifq	08:14	-100	-130
lerl03ihq	08:18	-200	-218
lerl03ijq	09:00	-400	-430
lerl03ilq	09:05	-600	-641
lerl03inq	09:09	-800	-858
lerl03ipq	09:13	-1000	-1065

Table 2. Log of exposures and focus offsets for G160M/1600 sweep across LP6.

Filename	Start Time (UT)	Relative Focus from LP6 (steps)	Breathing Corrected LP6 Focus (steps)
2021-12-31 – Estimated Absolute Focus : +78 steps			
FUVA + FUVB			
lerl04dtq	13:15	-1000	-1000
lerl04dvq	13:32	-800	-794
lerl04dxq	14:39	-600	-640
lerl04dzq	14:56	-400	-401
lerl04e1q	15:13	-100	-208
lerl04e3q	16:14	-200	-141
lerl04e5q	16:31	0	+3
lerl04e7q	16:48	+100	+93
lerl04e9q	17:49	+200	+155
lerl04ebq	18:07	+400	+400
lerl04edq	18:24	+600	+592
lerl04efq	19:25	+800	+760
lerl04ehq	19:42	+1000	+995

Table 3. 2D Image Extraction Regions

Grating	Segment	YCORR
G130M	FUVA	532 - 592
G130M	FUVB	593 - 653
G160M	FUVA	525 - 585
G160M	FUVB	585 - 645

3.1 Breathing Correction

Due to the thermal contraction and expansion of the HST optical telescope assembly (OTA) as the telescope warms up during its orbital day and cools down during orbital night, hereafter termed thermal breathing, corrections to the commanded focus positions are applied before determining the best focus position. This is because thermal breathing causes the actual focus position to be slightly offset from the commanded focus position. We apply a model of the breathing, based on temperatures measured by sensors aboard HST, to determine the breathing correction. This HST focus model tool [1] computes the focus offset, in microns, with respect to the nominal value at the time of a given observation. We note that the focus offset is derived for WFC3/UVIS1 data, and assume a similar application to COS observations. Using this tool, we determine the breathing-corrected focus offsets at the start of each exposure in the program, as shown in Figure 1. Multiplying micron focus offsets by 19.2 (see Oliveira et al. 2013) gives the breathing corrections in focus steps, which are then applied to the commanded focus values to calculate the corrected values where:

breathing-corrected focus offset = commanded focus offset - breathing correction

with final, corrected focus offset values listed in Tables 1 and 2.

4. Data Analysis

Following previous COS/FUV focus sweeps, we employ an auto-correlation method to determine the best-fit focus for each setting. Broad regions of FUV spectra which contain narrow absorption features are selected and auto-correlated with themselves, sampling a majority of the wavelength range covered in each grating and detector segment. Chosen wavelength ranges are listed in Table 4. The width of the auto-correlation function (ACF) provides a statistical measure of the widths of the absorption lines contained within each spectral region, and therefore also the spectral resolution and the focus, as a better focused instrument provides a narrower absorption line, which in turn provides a narrower ACF width. We calculate the ACF for each position in the focus sweep across each observed setting, normalized to unity at its peak, and measure the full width at half maximum (FWHM) of the ACF. Plotting the distribution of ACF widths as a function of corrected focus offset produces a focus curve, which is fit with a cubic function to determine its minimum.

4.1 G130M/1222 Sweeps

The focus curves for G130M/1222 are shown in Figure 2 with the focus offset providing the narrowest ACF width in each sweep listed in Table 4. The proposed best focus offset for G130M/1222 is not an average focus offset between the FUVA and FUVB

[1] https://focustool.stsci.edu

Table 4. Wavelength ranges $\delta\lambda$ used for auto-correlation analysis, and corresponding focus offsets (Δf) derived in each range.

Setting	$\delta\lambda(\AA)$	Δf
G130M/1222 FUVA	1250 - 1280, 1300 - 1350	-289
G130M/1222 FUVB	1130 - 1205	+69
Proposed Focus Offset		+70
G160M/1600 FUVA	1615 - 1666, 1673 - 1768	-29
G160M/1600 FUVB	1420 - 1524, 1528 - 1572	+94
Proposed Focus Offset		+30

values. Instead, we choose an offset of +70 steps, which optimizes the focus at shorter wavelengths accessible with FUVB, as it covers a unique and critical wavelength range available at typical G130M resolution only through this grating/cenwave set-up, similar to previous focus sweeps for this grating and cenwave (i.e. Fox et al. 2015). In doing so, we illustrate in Figure 2 that the difference in ACF width between the FUVA minimum and +70 steps is negligible. We adjust our estimated absolute focus value estimate by this offset to produce the final focus value using $f = f_{orig} + \Delta f$ to calculate $f = -881$ for the G130M/1222 grating set-up at LP6.

4.2 G160M/1600 Sweeps

The focus curves for G160M/1600 are shown in Figure 3 with the focus offset providing the narrowest ACF width in each sweep listed in Table 4. The proposed best focus offset for G160M/1600 at each position is the average focus offset between the FUVA and FUVB values. We measure focus offset values of $\Delta f = -29$ and +94 from the FUVA and FUVB focus curves, respectively, for final focus offset of $\Delta f = +30$. We adjust our estimated absolute focus value estimate by this offset to produce the final focus value using $f = f_{orig} + \Delta f$ to calculate $f = +108$ for the G160M/1600 grating set-up at LP6.

5. Results and Conclusions

The optimal focus value for G130M/1222 was found to be at the absolute COS/OSM1 focus steps of f = -881. Similarly, the optimal focus value for G160M/1600 was found to be at the absolute COS/OSM1 focus steps of f = +108.

These absolute values, also listed in Table 5, were supplied to the flight software table `Pcmech_OSMtbl`, which is found in the flight software file `pcmech.c`, for use in all subsequent G160M and G130M observations at cenwave 1222 at LP6. Subsequently updated focus values for the remaining G160M cenwaves are also included in Table

Table 5. Final Focus Values for G130M/1222 and G160M/ALL

Grating / Cenwave	Estimated Abs. f (steps)	Relative f Offset (steps)	Final Abs. f (steps)
G130M/1222	-951	+70	-881
G160M/1600	+78	+30	+108
—			
G160M/1533	—	—	-770
G160M/1577	—	—	-232
G160M/1589	—	—	-62
G160M/1611	—	—	+278
G160M/1623	—	—	+448

5, using focus offsets between each other cenwave and the 1600 cenwave applied in previous focus sweeps.

Acknowledgements

The authors would like thank Andy Fox for sharing IDL codes useful in the provided analysis and acknowledge the use of the HST Focus Model tool provided by Colin Cox.

Change History for COS ISR 2023-19

Version 1: 7 August 2023- Original Document

References

Fischer, T. et al. 2021, COS ISR 2021-07, ”Focusing on New COS FUV Lifetime Positions: G130M/1291 at LP5 G140L/800 at LP3”

Fox, A., Oliveira, C., Penton, S., et al. 2015, COS ISR 2015-01, “The COS/FUV Focus Sweep Program at Lifetime Position 3 (LENA2/13635)”

Fox, A., Penton, S., & Taylor, J. 2017, COS ISR 2017-17, “Focusing the COS/FUV G160M and G140L Gratings at Lifetime Position 4”

Ghavamian, P. 2012, COS ISR 2012-01, “COS FUV Focus Determination for the G140L Grating”

Heber, U., Reid, I. N., & Werner, K. 2000, A&A, 363, 198, ”Spectral analysis of multi-mode pulsating sdB stars. II. Feige 48, KPD 2109+4401 and PG 1219+534”

James, B., Fox, A. & Frazer, E., 2019, COS ISR 2019-06, ”Focusing the New COS/FUV Cenwave G160M/1533”

James, B. et al., COS ISR on LP6 Exploratory Phase, COS ISR 2023-15, ”LP6 Exploratory Study”

Lennon, D., Oliveira, C., Hartig, G., et al. 2010, COS ISR 2010-07, “SMOV: COS FUV Focus Determination”

Oliveira, C., Bostroem, A., & Osterman, S. 2013, COS ISR 2013-01, “Second COS

FUV LP Results from the Focus Sweep Enabling Program, FENA3 (12796)"
Sankrit, R., et al. 2019, COS ISR 2019-01, "Focus Sweep for the New COS/FUV Cenwave G140L/800"
Sonnentrucker, P., et al. 2017, COS ISR 2017-20, "Quick-check of the COS/FUV G130M Spectral Resolution at Lifetime Position 4"

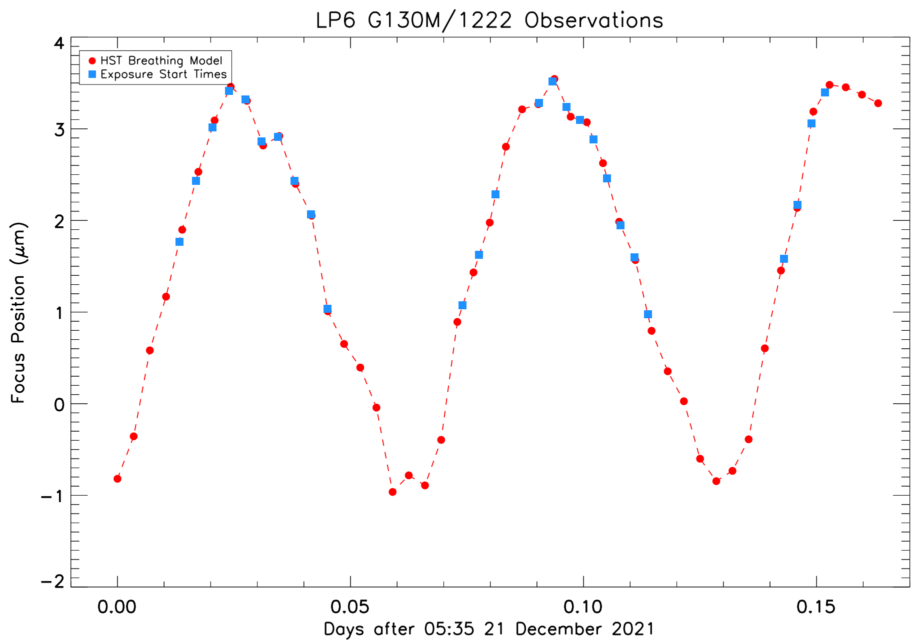

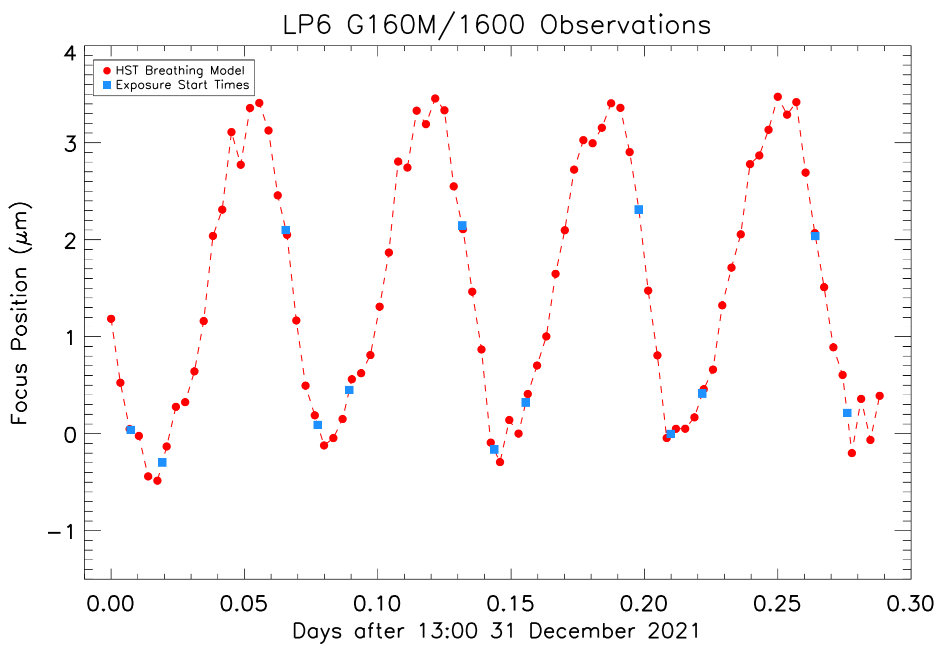

Figure 1. HST breathing models (red line) during the time when the G130M/1222 (top) and G160M/1600 (bottom) observations were taken. The distributions show the focus position in microns as a function of time. Each cycle has a period of one HST orbit and reflects the thermal breathing of the telescope. The breathing correction applied to each commanded relative focus offset, as shown in Tables 1 and 2, is directly proportional to the focus position at the time of observation.

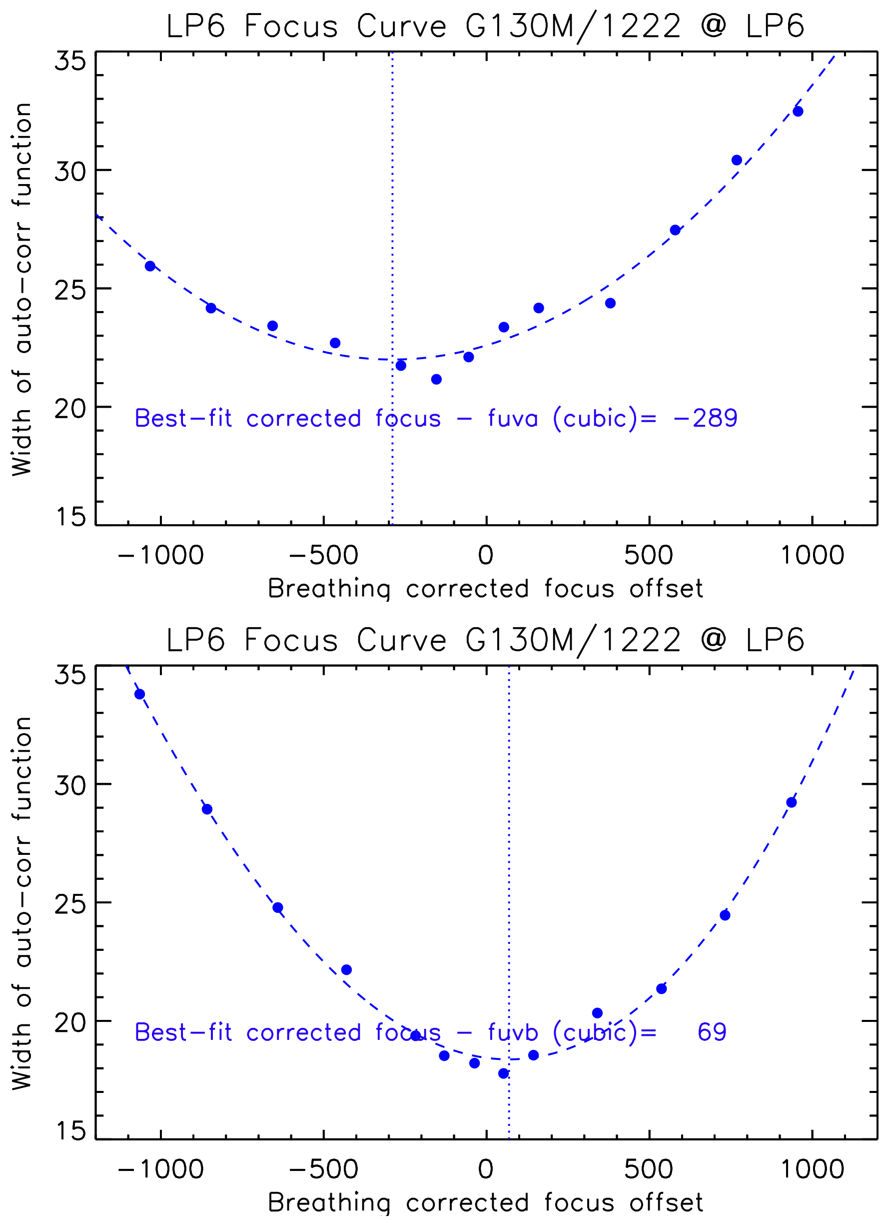

Figure 2. Focus curves across the FUVA (top) and FUVB (bottom) segments using the G130M/1222 setting at +6.5 arcsec. The width of the ACF is plotted against breathing-corrected focus offset in steps relative to the initial absolute focus estimate for each position. Cubic best-fits to the focus offsets and the minima of the cubic fits are shown with the dashed curves and dotted vertical lines, respectively.

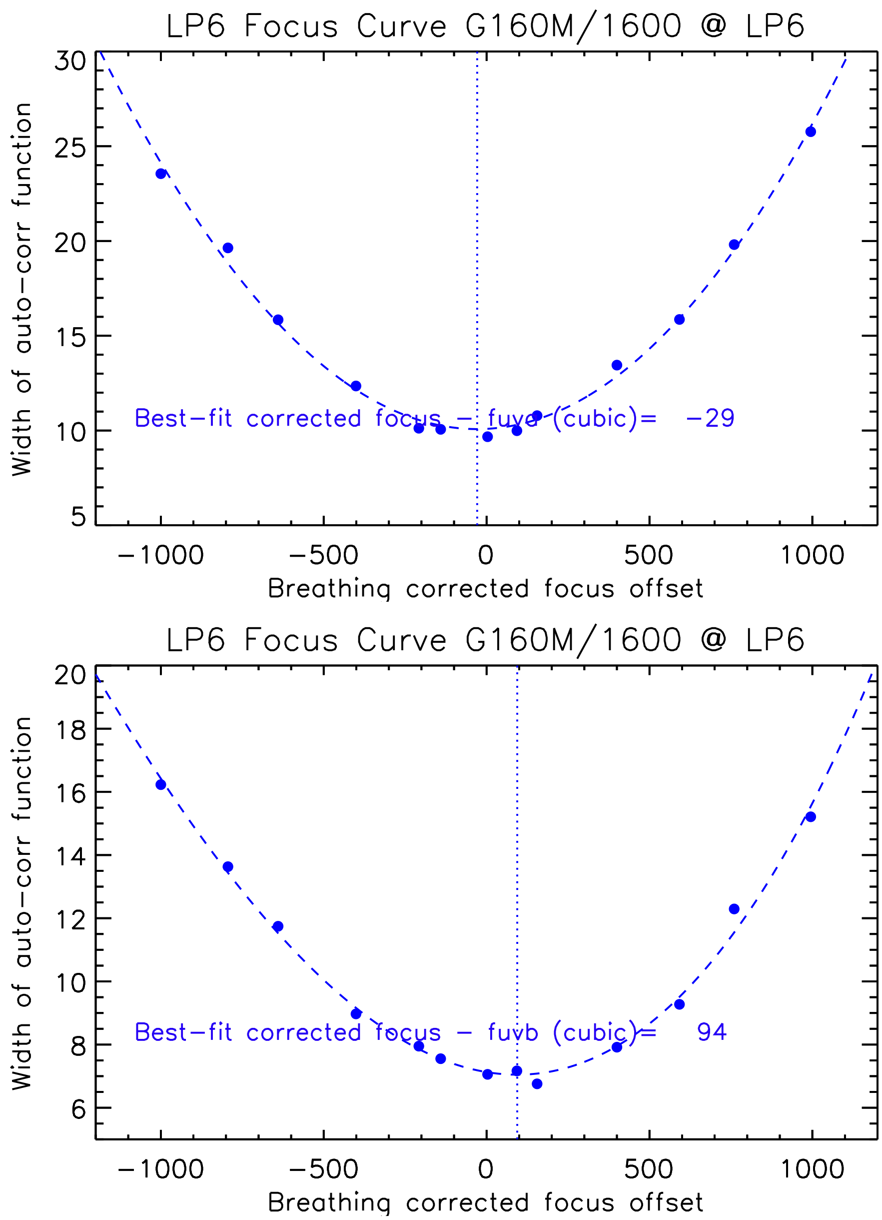

Figure 3. Focus curves across the FUVA (top) and FUVB (bottom) segment using the G160M/1600 setting at +6.5 arcsec. The width of the ACF is plotted against breathing-corrected focus offset relative to the initial absolute focus estimate for each position. Cubic best-fits to the focus offsets and the minima of the cubic fits are shown with the dashed curves and dotted vertical lines, respectively.